TECHNOLOGICAL UNIVERSITY DELFT

DEPARTMENT OF AERONAUTICAL ENGINEERING

Report VTH-124

THEORETICAL AND EXPERIMENTAL INVESTIGATIONS OF INCOMPRESSIBLE LAMINAR BOUNDARY LAYERS WITH AND WITHOUT SUCTION

Ph.D THESIS

J.L. van INGEN

DELFT
the NETHERLANDS

OCTOBER, 1965

This PDF-file contains chapter 5:

A new approximate method using the momentum equation for the calculation of boundary layers with and without suction

5. An approximate method using the momentum equation for the calculation of boundary layers with and without suction.

5.1. Introductory remarks.

In this chapter an approximate boundary layer calculation method, designed for application to suction problems will be described. A preliminary version of the method has been given in [65]. The essential point of the method is that an expression for the velocity profile is chosen which contains three important velocity profiles as special cases. These profiles are selected to be

the boundary layer on a flat plate without suction,
the asymptotic suction profile,
and the separation profile from the method of Timman.

The expression contains three parameters to be determined as functions of x from the momentum equation and the first and second compatibility condition at the wall. The method can be regarded as an extension of Schlichting's method discussed in section 4.3; the extension consists of adding the separation profile and the second compatibility condition. The results of the method are in good agreement with exact solutions without suction and with weak suction. For large values of the suction velocity the method breaks down because the expression selected for the velocity profile is not flexible enough to represent the wide class of velocity profiles, needed under greatly varying suction conditions. However, in most of the cases to be discussed in the present work the suction velocities will not be so high as to raise serious difficulties. The accuracy of the method may be assessed from the examples to be given in the present chapter and in chapters 8, 10 and 11.

5.2. The expression for the velocity profile and related parameters.

For the velocity profile the following expression is assumed:

$$\bar{u} = \frac{u}{U} = F_1(\eta) + K\, F_2(\eta) + L\, F_3(\eta) \qquad (5.1)$$

In this expression K and L are shape parameters; η is the non-dimensional wall distance defined by

$$\eta = \frac{y}{\sigma} \tag{5.2}$$

in which σ is a scaling factor related to the boundary layer thickness. The functions F_1, F_2 and F_3 are chosen in such a way that some special boundary layer velocity profiles are reproduced as accurately as possible for certain values of K and L. The functions F_1, F_2 and F_3 are defined by the equations (5.3) - (5.9)

$$F_1(\eta) = f_1(\eta) \tag{5.3}$$

$$F_2(\eta) = f_1(\eta) - f_2(\eta) \tag{5.4}$$

$$F_3(\eta) = f_1(\eta) - f_3(\eta) \tag{5.5}$$

with

$$f_1(\eta) = 1 - e^{a\eta} \tag{5.6}$$

$$f_2(\eta) = 2\,b\eta - 5(b\eta)^4 + 6(b\eta)^5 - 2(b\eta)^6 \quad \text{for } 0 \leqslant b\eta \leqslant 1 \tag{5.7}$$

$$f_2(\eta) = 1 \quad \text{for} \quad b\eta \geqslant 1 \tag{5.8}$$

$$f_3(\eta) = 1 - e^{-\eta^2} - \tfrac{1}{2}\,\eta^2\, e^{-\eta^2} \tag{5.9}$$

In these equations $\bar{u} = f_1(\eta)$ represents the asymptotic suction profile for $\frac{a}{\sigma} = \frac{v_o}{\nu}$; $f_2(\eta)$ is a good approximation of the Blasius profile (see section 5.4.2.) while $f_3(\eta)$ is the separation profile from Timman's method (section 4.3). The coefficients a and b are scaling factors which later on will be given the values 1.3 and 0.3 respectively. These values were determined in such a way that some important boundary layers different from the three mentioned above, will be reproduced as accurately as possible. This point is discussed in detail in section 5.8. The functions defined by equations (5.3) to (5.9) are shown in figure 5.1 for a = 1.3 and b = 0.3.

Using the expressions (5.3) to (5.9) and the definitions (2.17) and (2.18) for the displacement thickness δ^* and the momentum-loss thickness Θ it is found that

$$\frac{\delta^*}{\sigma} = p_1 + p_2\,K + p_3\,L \tag{5.10}$$

and

$$\frac{\theta}{\sigma} = p_4 + p_5 K + p_6 L + p_7 K^2 + p_8 L^2 + p_9\,KL \tag{5.11}$$

The coefficients p in (5.10) and (5.11) are rather complicated expressions in a and b containing error functions. For a = 1.3 and b = 0.3 the following values are obtained

$$\begin{aligned} p_1 &= 0.76923 & p_4 &= 0.38462 & p_7 &= -0.03938 \\ p_2 &= -0.18315 & p_5 &= -0.01925 & p_8 &= -0.10771 \\ p_3 &= -0.33855 & p_6 &= -0.01817 & p_9 &= -0.12361 \end{aligned} \tag{5.12}$$

Other important relations, to be used in what follows, are (see also the list of symbols)

$$\Lambda_1 = \bar{\theta}^2 \frac{d\bar{U}}{d\bar{x}} = \frac{\theta^2}{\nu}\frac{dU}{dx} = \frac{\sigma^2}{\nu}\frac{dU}{dx}\left(\frac{\theta}{\sigma}\right)^2 = \ell_1\left(\frac{\theta}{\sigma}\right)^2 \tag{5.13}$$

$$2 = \overline{v_o}.\bar{\theta} = \frac{-v_o\theta}{\nu} = \frac{-v_o\sigma}{\nu}\frac{\theta}{\sigma} = \ell_2\frac{\theta}{\sigma} \tag{5.14}$$

$$H = \frac{\delta^*}{\theta} = \frac{\delta^*/\sigma}{\theta/\sigma} \tag{5.15}$$

$$\ell = \frac{\tau_o\theta}{\mu U} = \frac{\theta}{\sigma}\frac{\tau_o\sigma}{\mu U} = \frac{\theta}{\sigma}\left(\frac{\partial\bar{u}}{\partial\eta}\right)_o = \frac{\theta}{\sigma}\left[\left(\frac{\partial F_1}{\partial\eta}\right)_o + K\left(\frac{\partial F_2}{\partial\eta}\right)_o + L\left(\frac{\partial F_3}{\partial\eta}\right)_o\right]$$

$$= \frac{\theta}{\sigma}\left[a + (a - 2b)K + aL\right] \tag{5.16}$$

For a = 1.3 and b = 0.3 the last relation becomes

$$\ell = \frac{\theta}{\sigma}(1.3 + 0.7\,K + 1.3\,L) \tag{5.17}$$

5.3. The momentum equation and compatibility conditions.

The present method employs the momentum equation (2.16) which, using the abbreviations given in the list of symbols, may be written in the form

$$\frac{d\bar{\theta}^2}{d\bar{x}} = \frac{2\ell - 2(2+H)\Lambda_1 - 2\Lambda_2}{\bar{U}} = \frac{M}{\bar{U}} \qquad (5.18)$$

In addition to (5.18) the first and second compatibility conditions (2.10) and (2.11) are used. These may be written as

$$-\ell_2 \left(\frac{\partial \bar{u}}{\partial \eta}\right)_o = \ell_1 + \left(\frac{\partial^2 \bar{u}}{\partial \eta^2}\right)_o \qquad (5.19)$$

$$-\ell_2 \left(\frac{\partial^2 \bar{u}}{\partial \eta^2}\right)_o = \left(\frac{\partial^3 \bar{u}}{\partial \eta^3}\right)_o \qquad (5.20)$$

Together with the expressions (5.3) to (5.9) defining the velocity profile, equations (5.19) and (5.20) lead to the following relations between K, L, ℓ_1 and ℓ_2.

$$K = \frac{-a\,\ell_2^2 - (a^2+1)\ell_1\ell_2 + a^3\ell_1 + a^3}{\ell_2^2(a - 2a^2b - 2b) + 2\,a^3b\,\ell_2 - a^3} \qquad (5.21)$$

$$L = \frac{2\,a^2b\,\ell_2^2 - 2\,a^3b\,\ell_2 + a^2\,\ell_1\ell_2 - a^3\ell_1}{\ell_2^2(a - 2\,a^2b - 2b) + 2\,a^3b\,\ell_2 - a^3} \qquad (5.22)$$

In (5.21) and (5.22) a and b should take the values 1.3 and 0.3 respectively. The boundary condition $\bar{u} = 1$ for $\eta \to \infty$ does not introduce additional relations between the parameters involved because this condition is satisfied already through the special choice for the functions $F_1(\eta)$, $F_2(\eta)$ and $F_3(\eta)$.

5.4. Similar solutions.

5.4.1. General.

For similar boundary layers the velocity profile - if suitably made non-dimensional - has to be independent of the streamwise coordinate x (section 3.1). Then, characteristic boundary layer parameters like ℓ and H become constants. In the present method this requires constant values for K and L and hence also Λ_1, Λ_2 and M should be independent of x.

Elimination of $\bar{\theta}$ from the following expressions

$$\Lambda_1 = \bar{\theta}^2 \frac{d\bar{U}}{d\bar{x}} \tag{5.23}$$

and

$$\frac{d\bar{\theta}^2}{d\bar{x}} = \frac{M}{\bar{U}} \tag{5.24}$$

leads to

$$\frac{\Lambda_1 \frac{d^2\bar{U}}{d\bar{x}^2}}{\frac{d\bar{U}}{d\bar{x}}} + \frac{M}{\bar{U}} \frac{d\bar{U}}{d\bar{x}} = 0 \tag{5.25}$$

Equation (5.25), in which M and Λ_1 are constants, defines the functions $\bar{U}(\bar{x})$ for which similar solutions may be obtained. Integration of (5.25) gives

$$\Lambda_1 \ln \left| \frac{d\bar{U}}{d\bar{x}} \right| + M \ln \bar{U} = \text{constant}$$

and after rearrangement

$$\text{constant} \cdot \bar{U}^{\frac{M}{\Lambda_1}} \, d\bar{U} = d\bar{x} \tag{5.26}$$

A second integration leads to

$$\bar{U} = c_1 e^{c_2 \bar{x}} \qquad \text{if} \qquad M = -\Lambda_1 \tag{5.27}$$

and to

$$\bar{U} = u_1 \bar{x}^{m_1} \qquad \text{if} \qquad M \neq -\Lambda_1 \tag{5.28}$$

In (5.27) and (5.28) c_1, c_2 and u_1 are irrelevant integration constants; m_1 is a constant defined by

$$m_1 = \frac{\Lambda_1}{\Lambda_1 + M} \tag{5.29}$$

Equations (5.27) and (5.28) show, that the present approximate method leads to the same permissible pressure distributions for the occurrence

of similar solutions as the exact theories, discussed in section 3.2. In what follows only the wedge-type flows, defined by (5.28) will be discussed further.

The permissible suction distribution is deduced from the requirement that also Λ_2 should be a constant. Then from (5.23) and

$$\Lambda_2 = \bar{v}_o \cdot \bar{\theta} \tag{5.30}$$

it follows, through elimination of $\bar{\theta}$, that

$$\bar{v}_o = \Lambda_2 \sqrt{\frac{\frac{d\bar{U}}{d\bar{x}}}{\Lambda_1}} \tag{5.31}$$

With (5.28) this leads to

$$\bar{v}_o = \Lambda_2 \sqrt{\frac{m_1 u_1}{\Lambda_1}}\, \bar{x}^{\frac{m_1-1}{2}} \tag{5.32}$$

which reproduces the exact result given by equation (3.13). In view of further use (5.32) may be rewritten in the form

$$\frac{-v_o}{U}\sqrt{\frac{Ux}{\nu}} = \frac{\Lambda_2}{\sqrt{\Lambda_1+M}} \tag{5.33}$$

5.4.2. The similar boundary layers for $\bar{U} = u_1 \bar{x}^{m_1}$ without suction.

For the similar boundary layer flows corresponding to (5.28) without suction Hartree's velocity profiles are obtained. (section 3.1.2.). In the present method these boundary layers are obtained as follows.
If suction is absent $\ell_2 = 0$ and the boundary layer parameters become functions of ℓ_1 only; they can easily be calculated using the formulae given in sections 5.2 and 5.3. The value of Hartree's parameter β then follows from (5.29) and (3.4).
Results of the calculations are given in fig. 5.2 where also a comparison

is made with the exact solution. Velocity profiles are shown in fig. 5.3 for the flat plate ($\beta = 0$) and the plane stagnation point ($\beta = 1$). Numerical values for some characteristic boundary layer parameters have been collected in table 5.1.

5.4.3. The plane stagnation point flow with suction.

It follows from section 3.1.4 that for the plane stagnation point flow $m_1 = 1$; then equation (5.29) shows that M should be zero. Due to this restriction only one independent parameter remains for which ℓ_2 will be selected. Inspection of (5.32) shows that, as a consequence of $m_1 = 1$, v_o is independent of $\bar{x}$. Some results of the present method for this case are collected in table 5.2; they are plotted as a function of $\lambda_2 = \frac{-v_o}{U}\sqrt{\frac{Ux}{\nu}}$ in fig. 5.4 and compared to exact solutions by Schlichting and Bussmann. (quoted by Mangler [37]).
Comparison with section 3.1.5 shows that both the exact and approximate solution tend to the asymptotic suction layer for $\lambda_2 \to \infty$.

5.4.4. The flat plate with $v_o \backsim x^{-\frac{1}{2}}$.

For a flat plate U is constant and hence from $\ell_1 = \frac{\sigma^2}{\nu}\frac{dU}{dx}$ it follows that $\ell_1 = 0$; equation (5.28) shows that also $m_1 = 0$. Equation (5.32) then indicates that for similar boundary layer flows v_o should be proportional to $x^{-\frac{1}{2}}$. From $\ell_1 = 0$ it follows that the boundary layer parameters are functions of ℓ_2 only in this case.
Results are given in fig. 5.5 and compared to exact solutions by Schlichting and Bussmann (quoted by Mangler [37]) and Thwaites [66];
Also for this case the boundary layer tends to the asymptotic suction layer for $\lambda_2 \to \infty$.

5.5. Step by step calculation of the boundary layer starting from given initial conditions.

In the boundary layer calculations it is assumed that $\bar{U}$, $\frac{d\bar{U}}{d\bar{x}}$ and $\bar{v}_o$ are known functions of $\bar{x}$. Furthermore at an initial station $\bar{x} = \bar{x}_o$ a starting

value for $\bar{\theta}$ should be known. (The determination of this starting value will be discussed in section 5.6).

For the step by step integration of the momentum equation (5.18) it is necessary to find M once $\bar{\theta}$ is known. This requires the knowledge of ℓ_1 and ℓ_2 which are determined by equations (5.13) and (5.14):

$$\Lambda_1 = \ell_1 \left(\frac{\theta}{\sigma}\right)^2 \tag{5.34}$$

$$\Lambda_2 = \ell_2 \frac{\theta}{\sigma} \tag{5.35}$$

where Λ_1 and Λ_2 are known from $\Lambda_1 = \bar{\theta}^2 \frac{d\bar{U}}{d\bar{x}}$ and $\Lambda_2 = \bar{v}_o.\bar{\theta}$. The relations between ℓ_1, ℓ_2 and $\frac{\theta}{\sigma}$ are rather complicated (see eqs. (5.11), (5.21) and (5.22) and it is not easy to solve (5.34) and (5.35) directly for ℓ_1 and ℓ_2. However, it was found that a simple iterative procedure can be used for this.

Starting from known values of Λ_1 and Λ_2 and an estimated value of $\frac{\theta}{\sigma}$, values of ℓ_1 and ℓ_2 are found from (5.34) and (5.35). Then K and L follow from (5.21) and (5.22) which determine an improved value of $\frac{\theta}{\sigma}$ using (5.11). Except very close to separation this process converges rapidly; in calculated typical examples each step in the iteration procedure increased the number of exact significant figures of $\frac{\theta}{\sigma}$ by one. The iteration should be stopped as soon as two consecutive values of $\frac{\theta}{\sigma}$ agree within a certain prescribed tolerance. Once this accuracy is achieved $\frac{\theta}{\sigma}$, ℓ_1 and ℓ_2 are known, satisfying (5.13) and (5.14). Then K and L follow from (5.21) and (5.22); $\frac{\delta^*}{\sigma}$ from (5.10); H from (5.15) and ℓ from (5.17). Now, all factors occurring in M are known and hence $\bar{\theta}$ at the next station can be found, etc. From the known values of K and L all boundary layer parameters and the velocity profile are known as functions of $\bar{x}$.

In all applications of the method, to be described in the present report, the iteration procedure outlined above was used. The step by step integration was performed by means of the four point Runge-Kutta method. In all cases the calculations were made on the Telefunken TR-4 digital computer of Delft Technological University.

It would be possible to speed up the calculation considerably if M were known directly as a function of Λ_1 and Λ_2 since then the iteration process could be left out. This can be achieved by plotting M on a large scale as function of Λ_1 and Λ_2 according to the formulae given in section 5.2 and 5.3. Fig. 5.7 shows a small scale version of such a plot. For use on a digital computer it would be necessary to feed the graph into the computer, either by fitting approximation formulae to the curves or by reading a table into the computer's memory. This method has not been used in the present work; for hand computation it would be an advantage to use the graph however.

A discussion of fig. 5.7 will be appropriate at this stage since it brings out clearly some characteristic features of the present method. The curve for $\Lambda_2 = 0$ corresponds to the case of zero suction and should be compared to fig. 4.1 for Pohlhausens $F(\Lambda_1)$ discussed in section 4.2; this will be pursued further in section 5.7.
Point P_1 corresponds to K = -1, L = 0 and hence represents the flat plate without suction; P_2 is given by K = 0, L = 0 and hence represents the asymptotic suction profile. Furthermore P_3 represents Timman's separation profile without suction for which K = 0 and L = -1.
Certain curves in fig. 5.7 represent a class of boundary layers. It has been mentioned already that all boundary layers without suction fall on the curve P_3P_4 for which $\Lambda_2 = 0$. Similarly P_1P_2, for which $\Lambda_1 = 0$, covers all flat plate boundary layers with arbitrary suction distributions. All plane stagnation point flows with suction, discussed in section 5.4.3 fall along P_2P_4.
The graph is closed on the upper left hand side by a curve which for $\Lambda_2 < 0.30$ denotes separation. For $\Lambda_2 > 0.30$ separation is not yet reached on the bounding curve but here double valued functions start to appear. To avoid this complication the calculations are deliberately stopped when this line is reached. Using the iteration process described above, the calculation stops automatically because the iteration fails to converge in this region. This difficulty is similar to the one mentioned in section 4.3 for Schlichting's method; in the present method the complication arises at larger values of Λ_2 than for

Schlichting's method.

From the similar solutions, already discussed and from some further examples to be given in chapters 8, 10 and 11 it is found that the present method can be used with some confidence for $0 \leqslant \Lambda_2 \leqslant 0.5$. This is not surprising since in the points P_1, P_2 and P_3 of fig. 5.8 this was ensured a priori by the choice for the functions F_1, F_2 and F_3. Furthermore a and b have been given such values (see also section 5.8) that the results along P_1P_2 and $P_3P_1P_4$ became as accurate as possible. The remarks given above about the accuracy of the method are not applicable to cases where large discontinuities in pressure gradient or suction velocity occur; for such problems the accuracy may be rather poor (cf. section 8.12).

5.6. Determination of the starting value for $\bar{\theta}$.

The boundary layer calculation has to start in the stagnation point where $\bar{U} = 0$. Hence it follows from (5.18) that in the stagnation point $\frac{d\bar{\theta}^2}{d\bar{x}} \rightarrow \infty$ unless $M = 0$. This means that the boundary layer starts as one of the plane stagnation point flows discussed in section 5.4.3.

From the relations given in table 5.2 and fig. 5.4 the starting values can be determined if $\bar{v}_o\left(\frac{d\bar{U}}{d\bar{x}}\right)^{-1}$ in the stagnation point is known. The value of $\bar{\theta}$ follows directly from the given value of Λ_1 by using $\Lambda_1 = \bar{\theta}^2 \frac{d\bar{U}}{d\bar{x}}$.

However, $\frac{d\bar{\theta}^2}{d\bar{x}}$ takes the undeterminate value $\frac{0}{0}$; this can be made determinate by applying L'Hopital's rule to eq. (5.18). The result is

$$\frac{d\bar{\theta}^2}{d\bar{x}} = \frac{\bar{\theta}^2 \frac{d^2\bar{U}}{d\bar{x}^2} \frac{\partial M}{\partial \Lambda_1} + \bar{\theta} \cdot \frac{d\bar{v}_o}{d\bar{x}} \cdot \frac{\partial M}{\partial \Lambda_2}}{\frac{d\bar{U}}{d\bar{x}}\left(1 - \frac{\partial M}{\partial \Lambda_1}\right) - \frac{\bar{v}_o}{2\bar{\theta}} \frac{\partial M}{\partial \Lambda_2}} \qquad (5.36)$$

where all values in (5.36) are to be taken in the stagnation point. In general suction will not be applied near the stagnation point because there is no tendency for transition or separation in this region. For the no-suction case (5.36) takes a simple form analogous to a relation

obtained for the Pohlhausen method ([7], chapter 12).

$$\left(\frac{d\bar{\theta}^2}{d\bar{x}}\right)_{st} = \frac{\bar{\theta}^2 \frac{d^2\bar{U}}{d\bar{x}^2} \frac{\partial M}{\partial \Lambda_1}}{\frac{d\bar{U}}{d\bar{x}}\left(1 - \frac{\partial M}{\partial \Lambda_1}\right)} = \frac{\Lambda_1 \frac{d^2\bar{U}}{d\bar{x}^2} \frac{\partial M}{\partial \Lambda_1}}{\left(\frac{d\bar{U}}{d\bar{x}}\right)^2\left(1 - \frac{\partial M}{\partial \Lambda_1}\right)} \qquad (5.37)$$

or with $\Lambda_1 = 0.08572$ and $\frac{\partial M}{\partial \Lambda_1} = -4.844$ in the stagnation point

$$\left(\frac{d\bar{\theta}^2}{d\bar{x}}\right)_{st} = -0.07105 \frac{\left(\frac{d^2\bar{U}}{d\bar{x}^2}\right)_{st}}{\left(\frac{d\bar{U}}{d\bar{x}}\right)^2_{st}} \qquad (5.38)$$

In general the step by step calculation will require short steps near the stagnation point; moreover for experimentally determined pressure distributions $\bar{U}$ and its derivatives will not be known with great accuracy near the stagnation point. Therefore it is recommended to start the step by step solution a small distance $\bar{x}_o$ away from the stagnation point. The starting value for $\bar{\theta}$ may then be found by applying one of the similar - or series solutions from $\bar{x} = 0$ to $\bar{x}_o$. For the case of zero suction the simple formulae (5.40) to be discussed in section 5.7 should be used.

It was found that for the typical case of an airfoil without suction the solution at larger distances from the stagnation point is rather insensitive to the starting values used. Therefore it appears that the calculation of the starting values may be rather inaccurate.

5.7. Simplification of the method for the no-suction case.

When no suction is applied eq. (5.21) and (5.22) show that $K = -1 - \ell_1$ and $L = \ell_1$; this leads to a considerable simplification because only one parameter (ℓ_1) occurs and the method becomes analogous to the Pohlhausen method. Important boundary layer parameters for $\ell_2 = 0$ have been given in table 5.3 as a function of ℓ_1; the results are plotted in fig. 5.6 as a function of Λ_1. Assuming a linear relationship between M and Λ_1 of the form

$$M = a_1 - b_1 \Lambda_1 \tag{5.39}$$

(compare Walz, section 4.2) the momentum equation (5.18) can be integrated from $\bar{x}_1$ to $\bar{x}_2$ giving

$$(\bar{U}^{b_1}\,\bar{\theta}^2)_{\bar{x}_2} - (\bar{U}^{b_1}\,\bar{\theta}^2)_{\bar{x}_1} = a_1 \int_{\bar{x}_1}^{\bar{x}_2} \bar{U}^{b_1-1}\, d\bar{x} \tag{5.40}$$

From an inspection of fig. 5.6 it is seen that for the present method the best values of a_1 and b_1 are as follows

region of applicability	a_1	b_1
near stagnation point (M = 0)	0.415	4.84
from stagnation point (M = 0) to pressure minimum (Λ_1 = 0)	0.437	5.10
from pressure minimum (Λ_1 = 0) to separation (Λ_1 = -0.087072)	0.437	6

For engineering applications the results will be sufficiently accurate if the values $a_1 = 0.437$ and $b_1 = 6$ are used all the way from stagnation point to separation.

Then, if the calculation is started in the stagnation point eq. (5.40) reduces to

$$\bar{U}^6\,\bar{\theta}^2 = 0.437 \int_0^{\bar{x}} \bar{U}^5\, d\bar{x} \tag{5.41}$$

5.8. Determination of the best values for a and b.

5.8.1. Determination of b.

In section 5.2 it was mentioned that a and b should take the values 1.3 and 0.3 respectively to obtain the best overall results of the present method. This may be discussed now in some more detail.

For boundary layer flows without suction it was found in section 5.7 that $K = -1-\ell_1$ and $L = \ell_1$. Hence (5.1) reduces to

$$\bar{u} = (1+\ell_1)\, f_2(\eta) - \ell_1\, f_3(\eta) \qquad (5.42)$$

showing that $f_1(\eta)$ and hence the coefficient a no longer occur in the expression for the velocity profile. Therefore the results of the present method, for boundary layers without suction, only depend on b.
For $\ell_1 = -1$ only the separation profile $f_3(\eta)$ is obtained, which is independent of b. For $\ell_1 = 0$ only $f_2(\eta)$ remains which gives the flat plate boundary layer without suction. The expressions (5.7) and (5.8) for $f_2(\eta)$ contain b but only as a scaling factor for y which does not influence the non-dimensional boundary layer parameters like ℓ, m, H etc. Hence both for $\ell_1 = 0$ and -1 the results of the present method are independent of b. For other values of ℓ_1 however they depend rather strongly on b. The best value of b was defined as the value which leads to the best representation of the Hartree profiles (cf. section 5.4.2). It was found that b = 0.30 should be taken to obtain this.

5.8.2. Determination of a.

Once a value for the scaling factor b has been chosen only the scaling factor a remains to be determined; this was done as follows.
For the flat plate with constant suction velocity $-v_o$ an exact solution has been given by Iglisch [67]. this solution will be discussed in chapter 8. The present approximate method was used to calculate the boundary layer for this case, using different values for a. By comparison with the exact solution it was found that a = 1.30 shows the best overall results.

Table 5.1: Some characteristic parameters for the flat plate (β=0) and the plane stagnation point (β=1).

Method	$\frac{\delta^*}{x}\sqrt{\frac{Ux}{\nu}}$		$\frac{\theta}{x}\sqrt{\frac{Ux}{\nu}}$		$H=\frac{\delta^*}{\theta}$		$\frac{\tau_o\theta}{\mu U}$	
	β=0	β=1	β=0	β=1	β=0	β=1	β=0	β=1
Pohlhausen	1.750	0.641	0.686	0.278	2.55	2.31	0.235	0.331
Schlichting	1.742	0.630	0.655	0.266	2.66	2.37	0.215	0.310
Timman	1.715	0.636	0.660	0.267	2.60	2.38	0.218	0.312
present	1.728	0.659	0.661	0.293	2.61	2.25	0.219	0.364
exact	1.721	0.648	0.664	0.292	2.59	2.21	0.221	0.360

Table 5.2: Results of the momentum method for the plane stagnation point with constant suction.

ℓ_2	ℓ_1	K	L	δ^*/σ	θ/σ	H	ℓ	Λ_1	Λ_2	λ_2
0	0.5835	-1.5835	0.5835	0.8617	0.3833	2.248	0.3642	0.08572	0.0000	0
0.1	0.5359	-1.5555	0.5843	0.8563	0.3842	2.229	0.3729	0.07910	0.03842	0.1366
0.2	0.4893	-1.5195	0.5821	0.8505	0.3851	2.209	0.3824	0.07256	0.07702	0.2859
0.3	0.4437	-1.4738	0.5761	0.8441	0.3862	2.186	0.3928	0.06620	0.1159	0.4504
0.4	0.3991	-1.4165	0.5652	0.8373	0.3872	2.162	0.4039	0.05983	0.1549	0.6333
0.5	0.3554	-1.3455	0.5482	0.8301	0.3881	2.139	0.4156	0.05352	0.1941	0.8392
0.6	0.3127	-1.2582	0.5239	0.8223	0.3889	2.114	0.4279	0.04728	0.2333	1.0731
0.7	0.2707	-1.1519	0.4904	0.8142	0.3896	2.090	0.4407	0.04109	0.2727	1.3453
0.8	0.2290	-1.0238	0.4460	0.8058	0.3900	2.066	0.4536	0.03483	0.3120	1.6711
0.9	0.1873	-0.8712	0.3887	0.7972	0.3900	2.044	0.4662	0.02849	0.3510	2.0794
1.0	0.1448	-0.6922	0.3166	0.7888	0.3896	2.025	0.4780	0.02198	0.3896	2.6271
1.1	0.1004	-0.4858	0.2281	0.7810	0.3886	2.010	0.4882	0.01516	0.4275	3.4728
1.2	0.0527	-0.2536	0.1224	0.7743	0.3870	2.001	0.4959	0.00789	0.4644	5.2297
1.3	0.0000	-0.0000	0.0000	0.7692	0.3846	2.000	0.5000	0.00000	0.5000	∞

Table 5.3: Some characteristic parameters of the momentum method for the no-suction case ($\Lambda_2 = 0$).

ℓ_1	θ/σ	δ^*/σ	H	$\ell = \frac{\tau_o \theta}{\mu U}$	Λ_1	$M(\Lambda_1)$
-1.3	0.26510	1.1544	4.3546	-0.047718	-0.091361	1.0657
-1.2	0.27556	1.1389	4.1330	-0.033067	-0.091120	1.0515
-1.1	0.28556	1.1233	3.9337	-0.017134	-0.089699	1.0302
-1.0	0.29508	1.1078	3.7542	0	-0.087072	1.0021
-0.9	0.30413	1.0922	3.5912	+0.018248	-0.083246	0.96738
-0.8	0.31272	1.0767	3.4430	0.037526	-0.078235	0.92672
-0.7	0.32083	1.0612	3.3077	0.057749	-0.072052	0.88036
-0.6	0.32848	1.0456	3.1831	0.078835	-0.064739	0.82876
-0.5	0.33566	1.0301	3.0689	0.10070	0.056334	0.77250
-0.4	0.34236	1.0145	2.9633	0.12325	-0.046883	0.71188
-0.3	0.34860	0.99900	2.8657	0.14641	-0.036457	0.64760
-0.2	0.35436	0.98346	2.7753	0.17009	-0.025114	0.58004
-0.1	0.35966	0.96792	2.6912	0.19422	-0.012936	0.50982
0	0.36449	0.95238	2.6129	0.21869	0	0.43738
+0.1	0.36885	0.93684	2.5399	0.24344	+0.013605	0.36334
+0.2	0.37274	0.92130	2.4717	0.26837	+0.027787	0.28822
+0.3	0.37616	0.90576	2.4079	0.29340	+0.042449	0.21258
0.4	0.37911	0.89022	2.3482	0.31845	0.057490	0.13694
0.5	0.38159	0.87468	2.2922	0.34343	0.072805	0.061872
0.6	0.38360	0.85914	2.2397	0.36826	0.088289	-0.012118
0.7	0.38514	0.84360	2.1904	0.39284	0.10383	-0.084493
0.8	0.38621	0.82806	2.1441	0.41711	0.11933	-0.15481

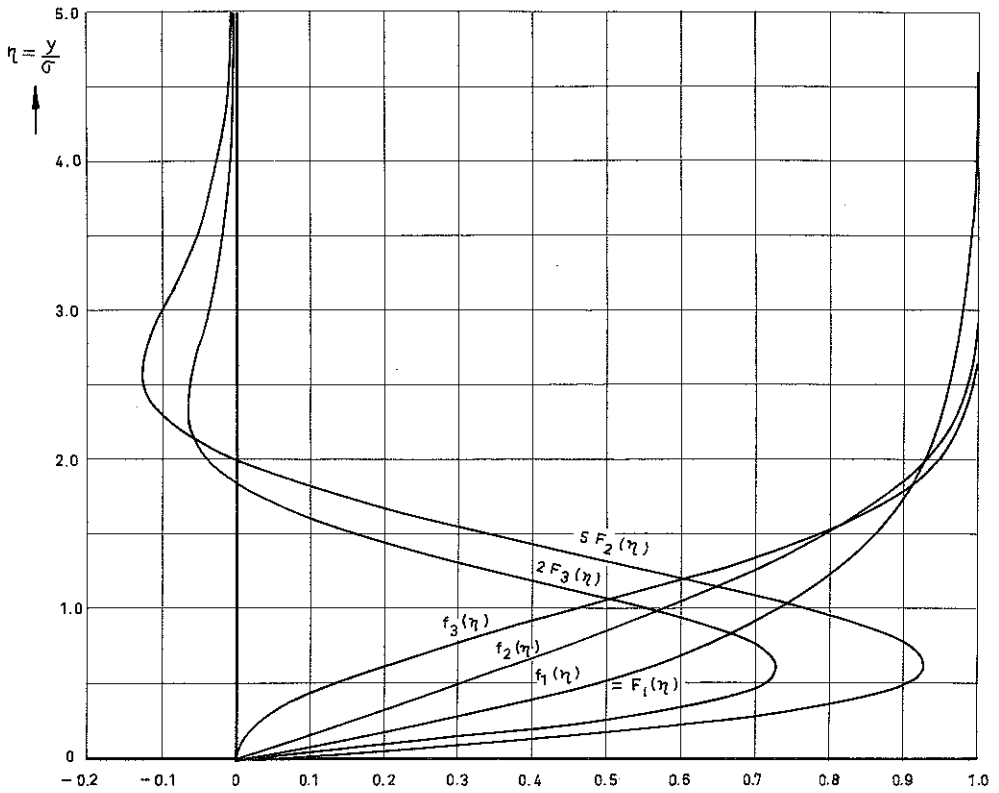

FIG. 5.1: THE FUNCTIONS DEFINED BY EQUATIONS (5.3) TO (5.9) FOR $a = 1.3$ AND $b = 0.3$

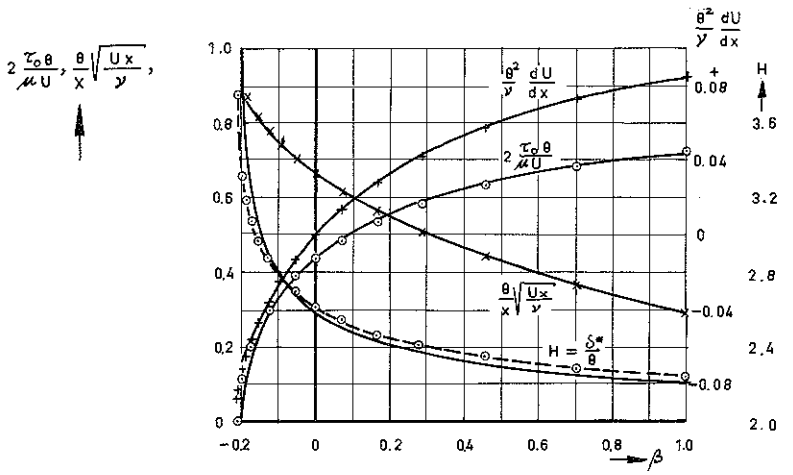

FIG. 5.2: RESULTS OF THE MOMENTUM METHOD FOR HARTREE'S BOUNDARY LAYERS.

——— exact Hartree — — — , +, x, ○ approximate method

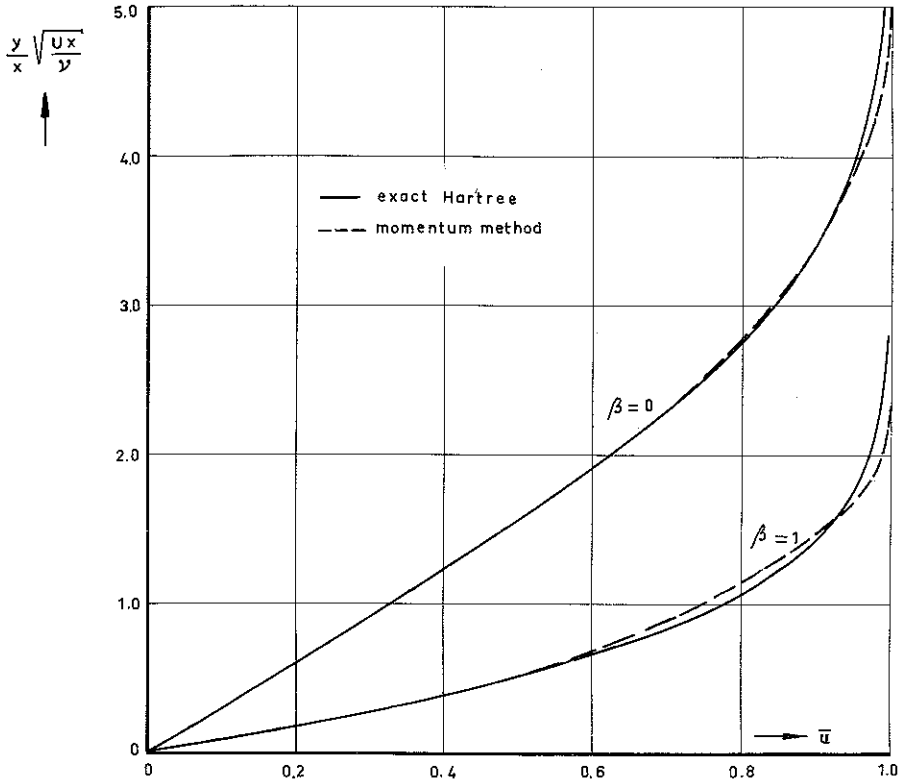

FIG. 5.3: VELOCITY PROFILES FOR THE FLAT PLATE ($\beta = 0$) AND THE PLANE STAGNATION POINT ($\beta = 1$), BOTH WITHOUT SUCTION.

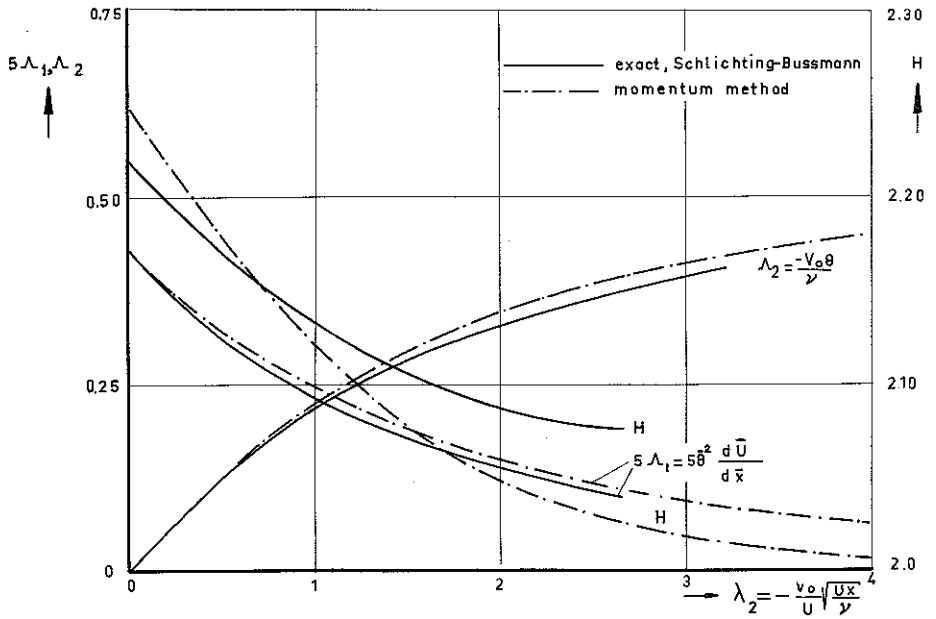

FIG.5.4: SOME RESULTS FOR THE PLANE STAGNATION POINT WITH CONSTANT SUCTION VELOCITY.

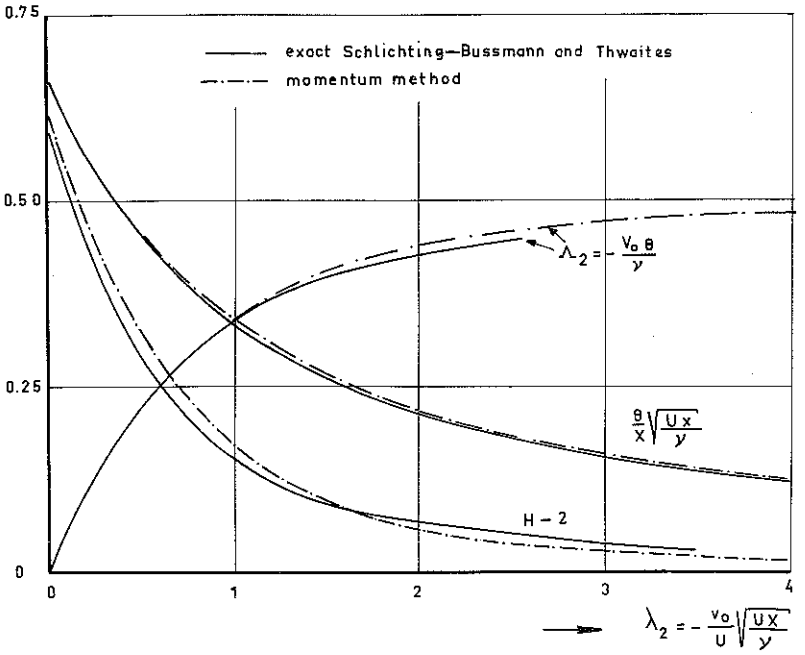

FIG. 5.5: SOME RESULTS FOR THE FLAT PLATE WITH $V_0 \infty x^{-1/2}$

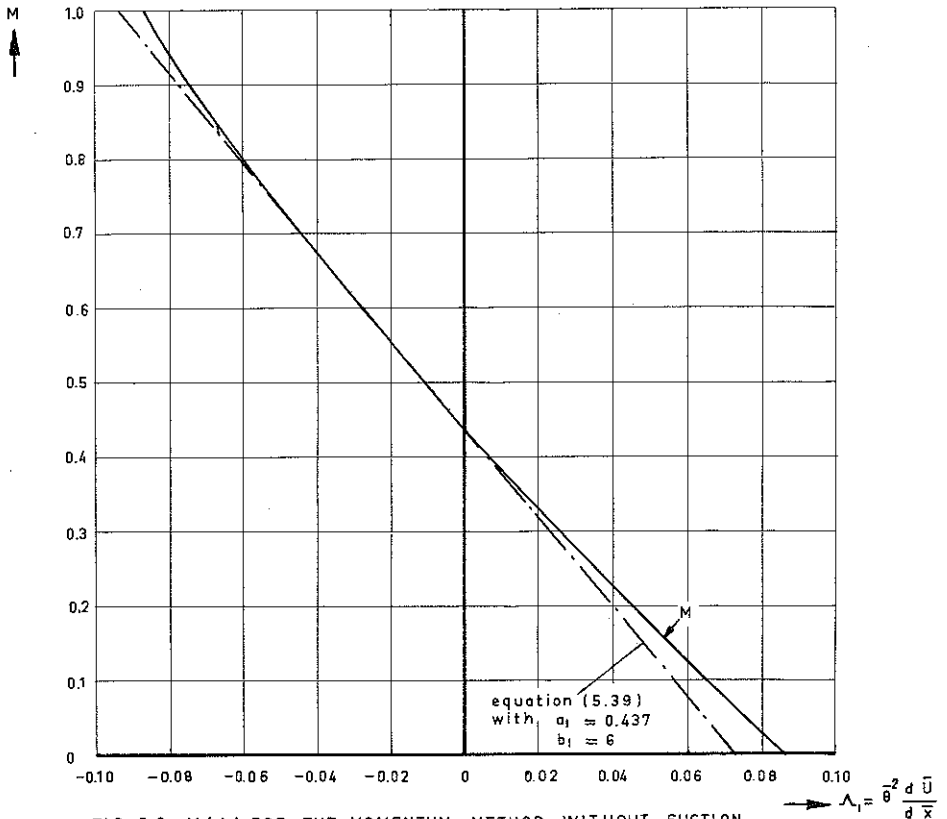

FIG. 5.6: $M(\Lambda_1)$ FOR THE MOMENTUM METHOD WITHOUT SUCTION

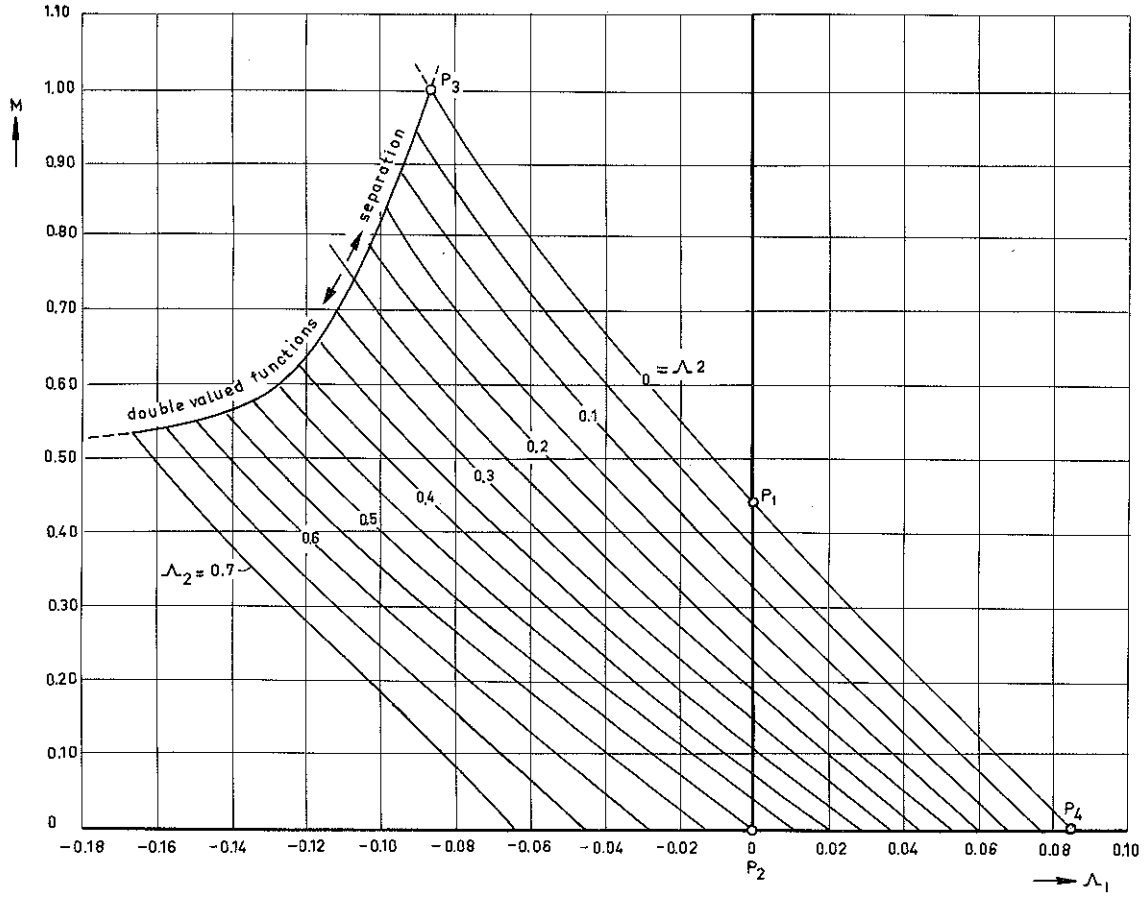

FIG. 5.7 : $M(\Lambda_1, \Lambda_2)$ FOR THE MOMENTUM METHOD.